ANTIOXIDANTS & REDOX SIGNALING
Volume 19, Number 5, 2013

DOI: 10.1089/ars.2011.4421

Therapeutics

ORIGINAL RESEARCH COMMUNICATION

Prx I Suppresses K-ras-Driven Lung Tumorigenesis by Opposing Redox-Sensitive ERK/Cyclin D1 Pathway

Young-Ho Park,[1,2,*] Sun-Uk Kim,[1–3,*] Bo-Kyoung Lee,[1,*] Hyun-Sun Kim,[1] In-Sung Song,[4] Hye-Jun Shin,[1,5] Ying-Hao Han,[1] Kyu-Tae Chang,[3] Jin-Man Kim,[6] Dong-Seok Lee,[1,7] Yeul-Hong Kim,[8] Chang-Min Choi,[9] Bo-Yeon Kim,[10] and Dae-Yeul Yu[1,2]

Abstract

Aims: Coupled responses of mutated K-ras and oxidative stress are often an important etiological factor in non–small-cell lung cancer (NSCLC). However, relatively few studies have examined the control mechanism of oxidative stress in oncogenic K-ras-driven NSCLC progression. Here, we studied whether the redox signaling pathway governed by peroxiredoxin I (Prx I) is involved in K-ras^{G12D}-mediated lung adenocarcinogenesis. ***Results:*** Using human-lung adenocarcinoma tissues and lung-specific K-ras^{G12D}-transgenic mice, we found that Prx I was significantly up-regulated in the tumor regions *via* activation of nuclear erythroid 2-related factor 2 (Nrf2) transcription. Interestingly, the increased reactive oxygen species (ROS) by null mutation of Prx I greatly promoted K-ras^{G12D}-driven lung tumorigenesis in number and size, which appeared to require the activation of the ROS-dependent extracellular signal-regulated kinase (ERK)/cyclin D1 pathway. ***Innovation:*** Taken together, these results suggest that Prx I functions as an Nrf2-dependently inducible tumor suppressant in K-ras-driven lung adenocarcinogenesis by opposing ROS/ERK/cyclin D1 pathway activation. ***Conclusion:*** These findings provide a better understanding of oxidative stress-mediated lung tumorigenesis. *Antioxid. Redox Signal.* 19, 482–496.

Introduction

Lung cancer is the leading cause of cancer-related deaths worldwide. Only 10%–15% of patients survive 5 years or longer (24). Lung cancer is classified into two major subtypes: small-cell and three types of non–small-cell lung cancer (NSCLC), including adenocarcinoma, squamous-cell carcinoma, and large-cell carcinoma (13). Among these four types, adenocarcinoma is the most common form of lung cancer, and ~30% of lung adenocarcinoma contains oncogenic single-point mutation at codons 12 or 13 of a K-ras (39). These K-ras mutations lead to uncontrolled cell division in human-lung adenocarcinoma (46, 51, 54). Thus, many studies have tried to treat lung tumorigenesis *via* modulation of oncogenic K-ras signaling pathways.

Ras-dependent downstream pathways include the Raf, mitogen-activated protein kinase kinase (MEK) and extracellular signal-regulated kinase (ERK), the aberrant activation of which ultimately leads to oncogenic transformation in numerous cancers by disrupting the control mechanism governing the cell cycle (8, 26). Thus, oncogenic K-ras mutation is closely associated with dysregulation of the cell-cycle

[1]Disease Model Research Laboratory, Aging Research Center, Korea Research Institute of Bioscience and Biotechnology, Daejeon, Korea.
[2]Department of Functional Genomics, University of Science and Technology, Daejeon, Korea.
[3]National Primate Research Center, Korea Research Institute of Bioscience and Biotechnology, Daejeon, Korea.
[4]Cardiovascular and Metabolic Disease Center, Inje University, Busan, Korea.
[5]College of Veterinary Medicine, Chungnam National University, Daejeon, Korea.
[6]College of Medicine, Chungnam National University, Daejeon, Korea.
[7]College of Natural Sciences, Kyungpook National University, Daegu, Korea.
[8]College of Medicine, Korea University, Seoul, Korea.
[9]College of Medicine, Ulsan University, Seoul, Korea.
[10]World Class Institute, Korea Research Institute of Bioscience and Biotechnology, Chungbuk, Korea.
*These authors contributed equally to this work.

Innovation

In this article, we present the data showing a critical role of reactive oxygen species (ROS) up-regulation in K-ras-induced lung tumorigenesis. Interestingly, K-ras mutation leads to up-regulation of peroxiredoxin I (Prx I) through activation of nuclear erythroid 2-related factor 2 (Nrf2), and we analyzed the cross-talk between Prx I and Nrf2, suggesting a novel feedback mechanism by ROS in lung cancer. Moreover, our findings illustrate an underlying mechanism by which Prx I suppresses lung tumorigenesis through the formation of a novel ROS/extracellular signal-regulated kinase (ERK)/cyclin D1 signaling pathway; therefore, Prx I has become an important target molecule for managing lung cancers, offering a new direction for therapeutic approaches.

machinery in a variety of tumors (16). Specifically, overexpression of cyclin D1, a representative K-ras target gene, is often linked to mutant K-ras-mediated oncogenic activity, tumor survival, and malignant progression (3, 37). Thus, it is important to define the signaling pathways from oncogenic K-ras to cyclin D1 to improve the therapeutic modality of NSCLC patients.

Peroxiredoxin I (Prx I) belongs to a special antioxidant family that regulates the responses to reactive oxygen species (ROS)-associated action, including cellular proliferation and differentiation (6, 17, 21). Recent evidence has shown that Prx I is closely related to tumor physiology, such as tumorigenesis (15, 41) and protection against therapeutic challenges (30, 59). In addition, Prx I is frequently up-regulated in a variety of cancer cells and tumors, appearing to be closely associated with the activation of nuclear erythroid 2-related factor 2 (Nrf2)/kelch-like ECH-associated protein 1 (Keap1) pathway in NSCLC. While evidence for an essential role of ROS in oncogenic K-ras-mediated tumorigenicity (2, 50, 57) is increasing, a few studies have examined the role of Prx I and its possible role in oncogenic K-ras-driven lung tumorigenesis.

In the current study, we have demonstrated that Prx I is up-regulated by oncogenic K-ras in a Nrf2/Keap1-dependent manner and that null mutation of Prx I promotes oncogenic K-ras-driven lung tumorigenesis *via* hyperactivation of the ROS/ERK/cyclin D1 pathway. These findings provide a better understanding of tumor-associated oxidative stress and may identify new therapeutic targets to treat K-ras-driven NSCLC patients.

Results

Prx I is up-regulated in human lung adenocarcinoma via activation of Nrf2

To investigate the role of Prx I in lung tumorigenesis, we examined Prx I expression using human-lung adenocarcinoma samples. As with PCNA, Prx I mRNA and protein was increased approximately threefold in lung tumors compared with nontumor tissues (Fig. 1A, B). Immunohistochemical data also showed that immunoreactivity to Prx I was greatly increased in the tumor regions of human patients with lung adenocarcinoma (Fig. 1C). These results are suggestive of a possible role of Prx I during lung-tumor progression.

To define the mechanism of Prx I up-regulation, we examined the expression of Nrf2, which is known as a key transcription factor for Prx I up-regulation (1, 5, 29). Compared with nontumor tissues, Nrf2 was significantly increased in lung adenocarcinoma samples; whereas Keap1, an inhibitor of Nrf2, was greatly reduced (Fig. 1D). To confirm the Nrf2 dependency of Prx I up-regulation, siRNA for Nrf2 (siNrf2) was transfected into A549 lung cancer cells and subjected to Western blotting analysis. Approximately 73% of Nrf2 expression was knocked down by transfection of siNrf2, which resulted in a decrease of Prx I as well as heme oxygenase-1 (HO-1), a representative Nrf2 target gene (Fig. 1E). These results suggest that Prx I is up-regulated during lung-tumor progression in an Nrf2-dependent manner.

K-ras mutation leads to up-regulation of Prx I through activation of Nrf2 in lung adenocarcinoma

K-ras mutation is known as an etiological factor causing lung adenocarcinoma. To investigate the relationship between K-ras oncogenic mutation and Prx I up-regulation, immunohistochemistry was carried out using transgenic mice with lung-specific expression of K-ras^{G12D} (K-ras^{G12D}-Tg mice) (34). Interestingly, Prx I expression was significantly increased in the lung tumor regions of K-ras^{G12D}-Tg mice (Fig. 2A) and human adenocarcinoma tissues with mutant K-ras (Supplementary Fig. S1; Supplementary Data are available online at www.liebertpub.com/ars). Consistent with this, overexpression of K-ras^{G12D} greatly increased the transcript levels of Prx I and Nrf2 in HBEC3 cells, normal bronchial epithelial cell line (Supplementary Fig. S6D). In contrast, transfection of siK-ras greatly decreased Prx I expression in human NSCLC cell lines, such as A549 and NCI-H358 cells, with spontaneous K-ras mutation (Fig. 2B, C). Furthermore, Nrf2 and its target gene were decreased in expression on siK-ras transfection compared with cells transfected with control siRNA in A549 and NCI-H358 cells (Fig. 2D). These results indicate that the K-ras mutation induces the up-regulation of Prx I *via* activation of the Nrf2 pathway in NSCLC.

Null mutation of Prx I accelerates lung tumorigenesis in K-ras^{G12D}-Tg mice

To investigate whether activation of Prx I influences K-ras^{G12D}-driven lung tumorigenesis, we generated mutant mice carrying a null mutated Prx I gene and/or a K-ras^{G12D} transgene by breeding Prx I$^{-/-}$ mice and K-ras^{G12D}-Tg mice (Fig. 3A, B). Although these four genotypes of mice were similar in body and lung weights at 9 weeks of age (Supplementary Fig. S2A), histological analysis revealed that K-ras^{G12D}-mediated tumorigenesis was significantly increased by knockout of Prx I (Fig. 3C–E). Consistently, the tumors were significantly increased in both number and size in 7-month-old Prx I$^{-/-}$/K-ras^{G12D}-Tg mice compared with wild-type (WT)/K-ras^{G12D}-Tg animals (Supplementary Fig. S2B, C).

To further define the roles of Prx I in K-ras^{G12D}-driven lung tumorigenesis, we established 3T3-like mouse embryonic fibroblasts (3T3-MEFs) from WT and Prx I$^{-/-}$ fetuses and stably transfected them with the K-ras^{G12D} expression vector (Fig. 4A). Overexpression of K-ras^{G12D} enhanced anchorage-dependent or -independent growth in both genotype cells, which was most notable in Prx I$^{-/-}$ 3T3-MEFs compared with other genotypes (Fig. 4B–D). In addition, siPrx

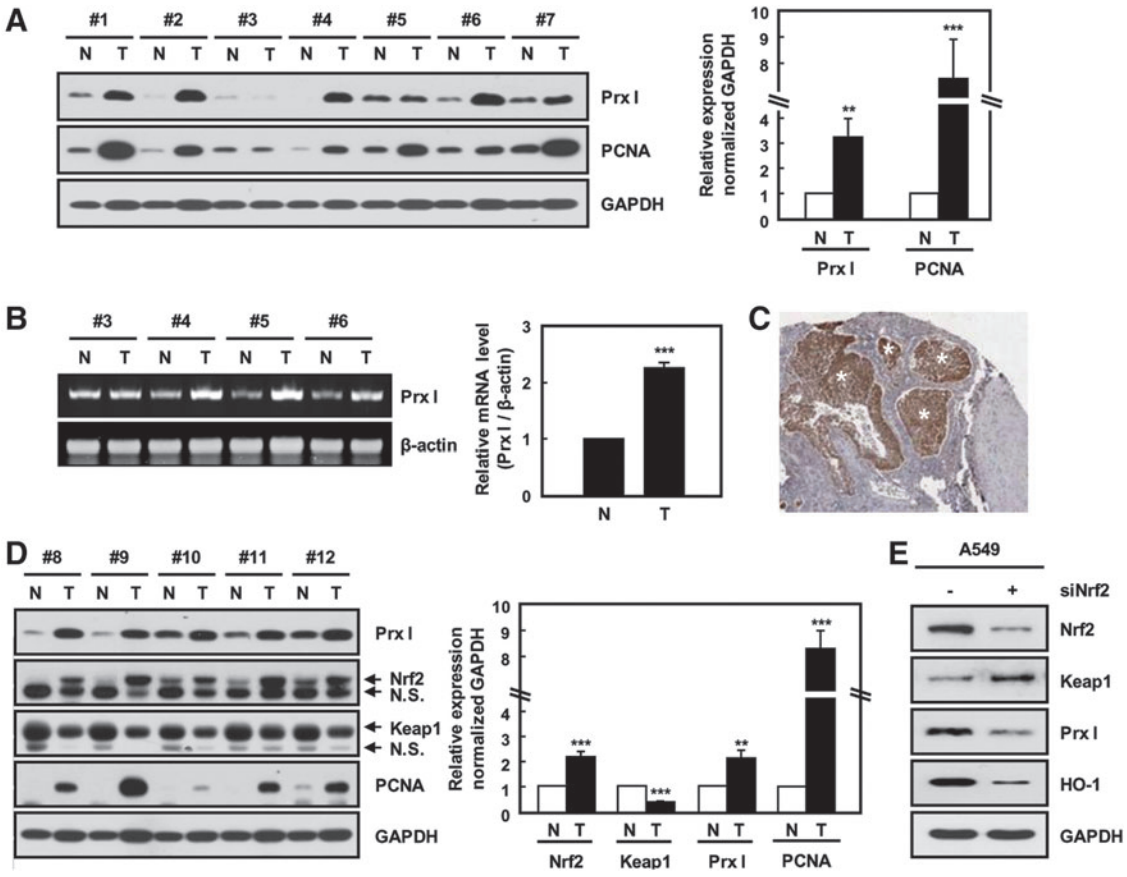

FIG. 1. Elevated expression of Prx I and Nrf2 in human-lung adenocarcinoma tissues. (A) Relative expression levels of Prx I and PCNA in paired nontumor (N) and tumor (T) tissue samples from seven patients with adenocarcinoma were determined by Western blotting analysis. GAPDH was used as a loading control. The data are presented as the mean ± SEM ($n = 7$). $^{**}p < 0.01$, $^{***}p < 0.001$ compared with paired nontumor tissue samples. **(B)** Prx I mRNA level in lung cancer tissues was measured by semi-quantitative PCR. The data are representative of at least three different experiments and presented as mean ± SEM ($n = 4$). $^{***}p < 0.001$ compared with paired nontumor tissue samples. **(C)** Human lung adenocarcinoma tissue sections were prepared and stained with anti-Prx I antibody. *Asterisks* indicate tumor regions. **(D)** Relative expression levels of Nrf2 and Keap1 in five patients with adenocarcinoma were determined by Western blotting analysis. The data are representative of at least three different experiments and presented as mean ± SEM ($n = 14$). $^{**}p < 0.01$, $^{***}p < 0.001$ compared with paired nontumor tissue samples. **(E)** Nrf2 and Prx I expression in siNrf2-transfected A549 cells. The data are representative of at least three different experiments. Nrf2, nuclear erythroid 2-related factor 2; Prx I, peroxiredoxin I; siNrf2, siRNA for Nrf2. To see this illustration in color, the reader is referred to the web version of this article at www.liebertpub.com/ars

I-transfected A549 and NCI-H358 cells, a human NSCLC cell line, displayed a significant increase in anchorage-dependent or -independent growth (Supplementary Fig. S3A, B, respectively). These results strongly suggest that Prx I functions as a tumor suppressant in K-ras^{G12D}-driven lung tumorigenesis.

Prx I inhibits K-ras^{G12D}-driven tumorigenesis by neutralization of ROS

ROS generation is essential for oncogene-mediated tumorigenicity to activate critical signaling pathways that promote cellular proliferation (38, 57). Therefore, we investigated the potential contribution of Prx I-dependent signaling to inhibit ROS in oncogenic K-ras-driven tumorigenesis. WT and Prx I$^{-/-}$ 3T3-MEFs were stably transfected with the K-ras^{G12D} transgene, incubated with CM-H_2DCFDA, and subjected to flow cytometry. ROS level was greatly increased in Prx I$^{-/-}$ 3T3-MEFs compared with WTs, which was further elevated by the stable transfection of K-ras^{G12D} vector in both genotypes (Fig. 5A). Among the genotypes analyzed, the highest ROS level was detected in K-ras^{G12D}/Prx I$^{-/-}$ 3T3-MEFs (Fig. 5A). In contrast, overexpression of human Prx I using an adenoviral vector reduced the ROS level in K-ras^{G12D}/Prx I$^{-/-}$ 3T3-MEFs (Fig. 5B, C) and significantly ameliorated the anchorage-independent growth of K-ras^{G12D}/Prx I$^{-/-}$ 3T3-MEFs (Fig. 5D). Consistent with this, N-acetyl L-cysteine (NAC), a chemical antioxidant, greatly inhibited anchorage-independent growth of K-ras^{G12D}/Prx I$^{-/-}$ 3T3-MEFs (Fig. 5E). These results imply that Prx I participates in inhibition of oncogenic K-ras-driven tumorigenesis through its peroxidase activity.

Prx I inhibits oncogenic K-ras-mediated cell growth by suppressing the ROS/ERK/cyclin D1 pathway

Recent evidence has shown that oncogenic K-ras is known to control ERK activation and cyclin D1 expression (12, 19). Consistent with this, we found that K-ras knockdown in both A549 and NCI-H358 cells decreased the levels of both ERK

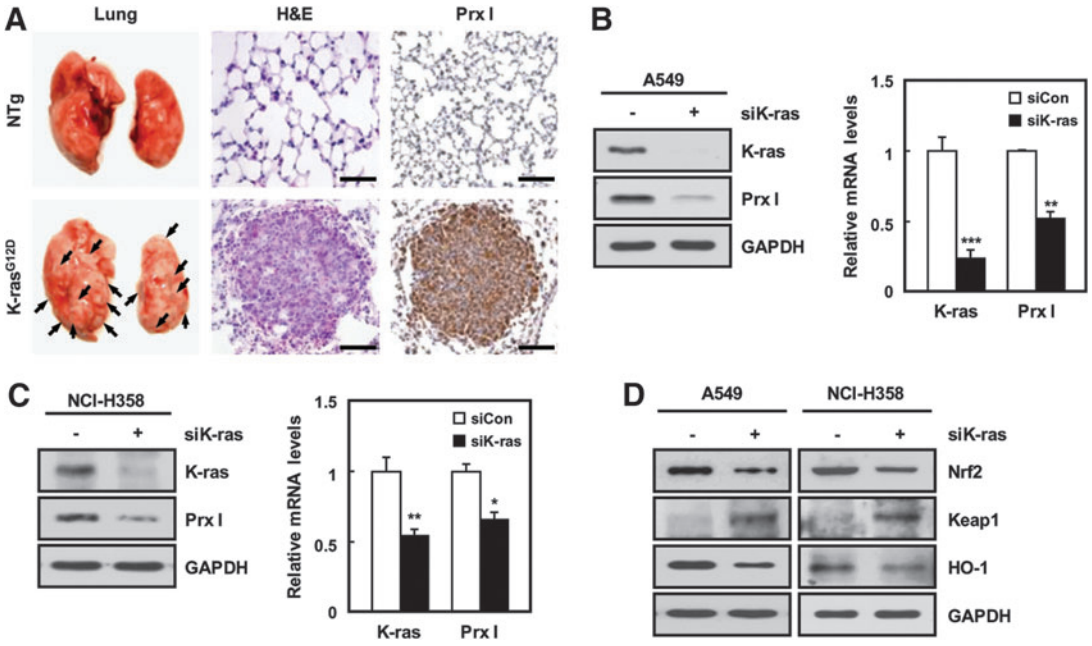

FIG. 2. Prx I is up-regulated by an oncogenic K-ras *via* the Nrf2 transcription factor. (A) H&E and anti-Prx I were stained in lung tissues of non-Tg (NTg) and K-ras^{G12D}-driven lung cancer model mice (K-ras^{G12D}-Tg) at 3 months. Tumors are indicated by *black arrows* on the lung surface (Scale bars, 50 μm). **(B, C)** Expression levels of K-ras and Prx I in siK-ras-transfected A549 and NCI-H358 cells were analyzed by Western blotting and quantitative PCR (qPCR) analyses. GAPDH was used as a loading control. The data are representative of at least three different experiments and presented as mean ± SEM. $^{*}p<0.05$, $^{**}p<0.01$, and $^{***}p<0.001$ compared with the cells transfected with scrambled siRNA. **(D)** Western blots were performed for Nrf2, Keap1, and HO-1 in siK-ras-transfected A549 and NCI-H358 cells. The data are representative of at least three different experiments. HO-1, heme oxygenase-1; Tg, transgenic. To see this illustration in color, the reader is referred to the web version of this article at www.liebertpub.com/ars

phosphorylation and cyclin D1 expression compared with control groups (Supplementary Fig. S4A). This result is suggestive of the ERK/cyclin D1 pathway as a downstream signal pathway of oncogenic K-ras in NSCLC. Interestingly, phosphorylation of ERK, but not JNK and p38 (Supplementary Fig. S4B, C), was markedly increased along with the increment of cyclin D1 protein and mRNA in Prx I$^{-/-}$ 3T3-MEFs and siPrx I-transfected A549 and NCI-H358 cells compared with the respective control cells (Fig. 6A–C and Supplementary Fig. S4D). Conversely, overexpression of Prx I in A549 cells inhibited ERK phosphorylation and cyclin D1 levels (Fig. 6D). This suggests the involvement of Prx I in oncogenic K-ras-mediated ERK/cyclin D1 cascade activation.

To test whether ROS participate in the modulation of ERK/cyclin D1 pathway in NSCLC cells with oncogenic K-ras expression, A549 cells were exposed to NAC or ERK signaling inhibitors, including PD98059 and U0126, and subjected to Western blotting analysis. Interestingly, ERK phosphorylation and cyclin D1 expression were significantly decreased by the addition of either NAC or ERK signaling inhibitors in A549 cells (Fig. 6E–G), suggesting the involvement of an ROS in K-ras^{G12D}/ERK/cyclin D1 signaling pathway. In addition, cell proliferation rate was greatly decreased by inhibition of the ERK signaling pathway in NCI-H358 cells and K-ras^{G12D}/Prx I$^{-/-}$ 3T3-MEFs (Fig. 7A, B). Moreover, overexpression of Prx I greatly reduced ROS in A549 cells (Fig. 7C), which ultimately resulted in reduction of the cell proliferation rate (data not shown) and anchorage-independent growth (Fig. 7D). Consistent with these results, tumor growth in nude mice was significantly suppressed by overexpression of Prx I in A549 cells (Supplementary Fig. S5). Together with ERK activation by the absence of Prx I in 3T3-MEFs, as shown in Figure 6A, these results strongly suggest that Prx I involves suppression of oncogenic K-ras-driven tumor growth by opposing ROS-dependent ERK/cyclin D1 cascade activation.

Oncogenic K-ras-dependent signaling pathways were highly activated in Prx I$^{-/-}$/K-ras^{G12D}-Tg mice

Similar to the data from NSCLC cell lines and MEFs, immunoreactivities against anti-Prx I, pERK, cyclin D1, and PCNA antibodies were mainly detected in the tumor regions of K-ras^{G12D}-Tg mice (Fig. 8A), and null mutation of Prx I dramatically increased the number of cells with high immunoreactivity to pERK, cyclin D1, and PCNA compared with WT/K-ras^{G12D}-Tg animals (Fig. 8A, B). Consistent with the results, Western blotting analysis also showed that ERK phosphorylation was dramatically increased in Prx I$^{-/-}$ lung tissues compared with WT, which was more increased in K-ras^{G12D}-Tg lung tissues than in NTg. Ultimately, ERK phosphorylation and cyclin D1/PCNA up-regulation were most notably found in the lung tissues of Prx I$^{-/-}$/K-ras^{G12D}-Tg mice compared with the other genotype animals (Fig. 8C). In particular, lung adenocarcinoma, a high-grade lung tumor, was predominantly found in Prx I$^{-/-}$/K-ras^{G12D}-Tg mice (Fig. 9A and Supplementary Table S1). Thus, the size and weight of lung tissues were markedly increased in Prx I$^{-/-}$/K-ras^{G12D}-Tg mice compared with WT/K-ras^{G12D}-Tg animals (Fig. 9B). Importantly, the median survival was more rapidly decreased in Prx I$^{-/-}$/K-ras^{G12D}-Tg mice than in

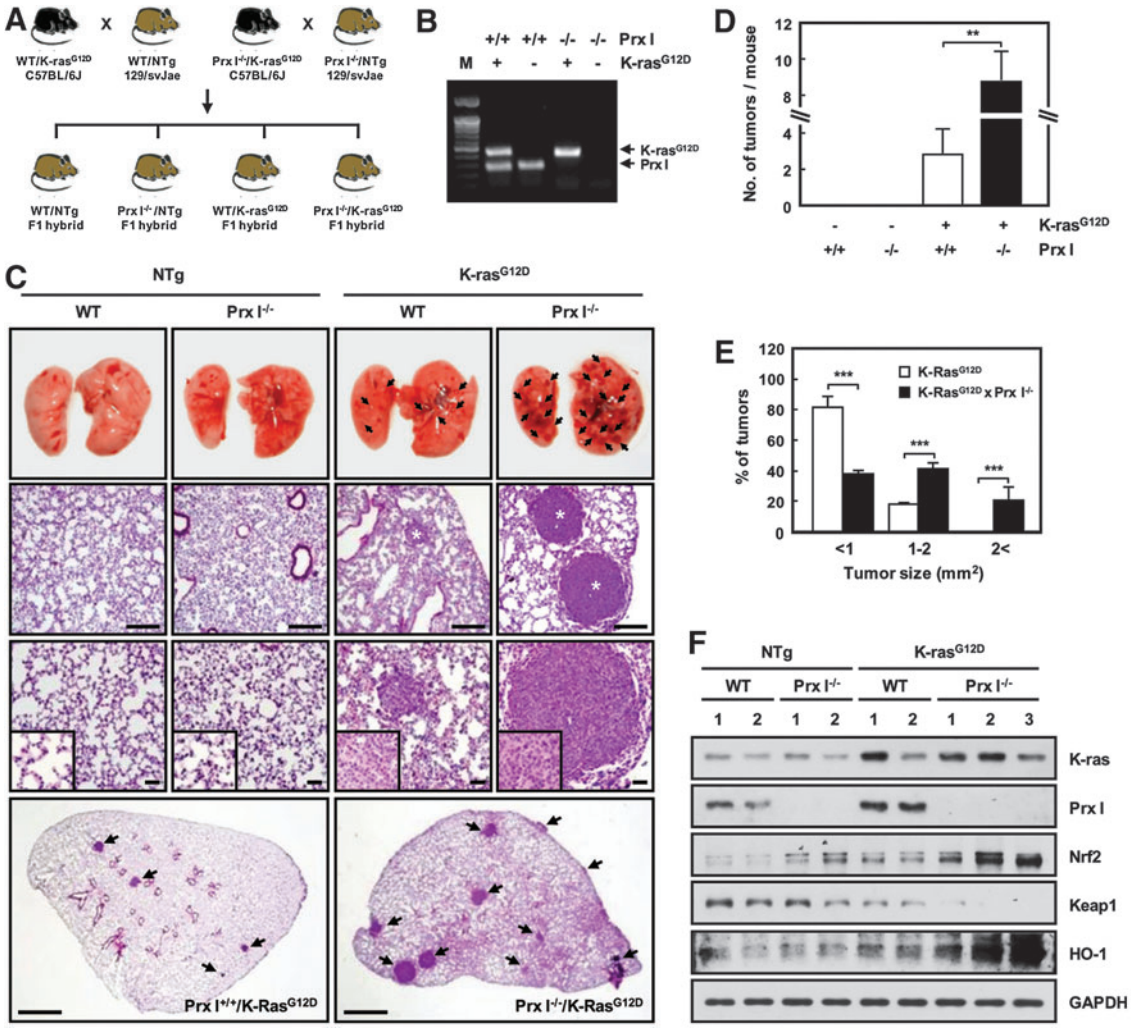

FIG. 3. Acceleration of lung tumorigenesis in Prx I$^{-/-}$/K-ras^{G12D}-Tg mice. (A) Schematic diagram of the breeding strategy. WT/K-ras^{G12D}-Tg and Prx I$^{-/-}$/K-ras^{G12D}-Tg mice were obtained by crossing B6129F1 (C57BL6/J×129/svj) mice carrying the K-ras^{G12D} and Prx I$^{-/-}$ alleles. **(B)** Genotyping of NTg, WT/K-ras^{G12D}-Tg, Prx I$^{-/-}$, and Prx I$^{-/-}$/K-ras^{G12D}-Tg mice by PCR experiments. The littermates served as NTg controls in all the experiments. **(C)** H&E stained sections of typical lesions in lungs from four groups of mice at 9 weeks (Scale bars, 50 μm). Tumors are indicated by *black arrows* and *white asterisks*. *Bottom panel* is a low-magnification image of WT/K-ras^{G12D}-Tg and Prx I$^{-/-}$/K-ras^{G12D}-Tg mice. Insets show representative histology in high magnification. Tumor number **(D)** and tumor size **(E)** in lungs from WT ($n=10$), WT/K-ras^{G12D}-Tg ($n=8$), Prx I$^{-/-}$ ($n=10$), and Prx I$^{-/-}$/K-ras^{G12D}-Tg ($n=11$) mice at 9 weeks. The data are presented as mean±SEM. $^{**}p<0.01$, $^{***}p<0.001$ compared with WT/K-ras^{G12D}-Tg mice. **(F)** Western blots for K-ras, Prx I, Nrf2, Keap1, and HO-1 in lungs from WT ($n=2$), Prx I$^{-/-}$ ($n=2$), WT/K-ras^{G12D}-Tg ($n=2$), and Prx I$^{-/-}$/K-ras^{G12D}-Tg ($n=3$) mice at 7 months. WT, wild type. To see this illustration in color, the reader is referred to the web version of this article at www.liebertpub.com/ars

WT/K-ras^{G12D}-Tg animals (Fig. 9C). From the data produced *in vitro* and *in vivo*, we conclude that Prx I acts as an inducible tumor suppressant in NSCLC tumorigenesis through impediment of oncogenic K-ras-dependent redox signaling pathways.

Discussion

Numerous pathological conditions, including inflammation, aging, and cancer, involve an ROS shift, which is closely associated with progression of diseases (48). To find the mechanism governing the modulation of enhanced oxidative stress, a variety of antioxidant defense systems, including Prxs, have been studied using numerous cancer cells and tissues (4, 36). From the protective role of Prxs against cancer therapeutic challenges, such as cancer drugs, ionizing radiation, and pro-oxidants (30, 60), many researchers have suggested that Prx can serve as a target molecule for improvement of anticancer activity (25). However, a better understanding of the role of Prx I and its underlying mechanism(s) in cancer is in need of additional detailed experiments.

The most remarkable biochemical function of Prxs is to scavenge ROS or peroxides (18, 23). Recent evidences have revealed that ROS function as second messengers in a variety of biological events, including tumorigenesis (33, 49). Indeed, numerous Prx isotypes, including Prx IV, involve the signaling pathways triggered by growth factors, such as granulocyte colony-stimulating factor and platelet-derived growth factor, *via* interaction with their receptors (11, 42). In these cascades, Prxs actively participates in the scavenging of

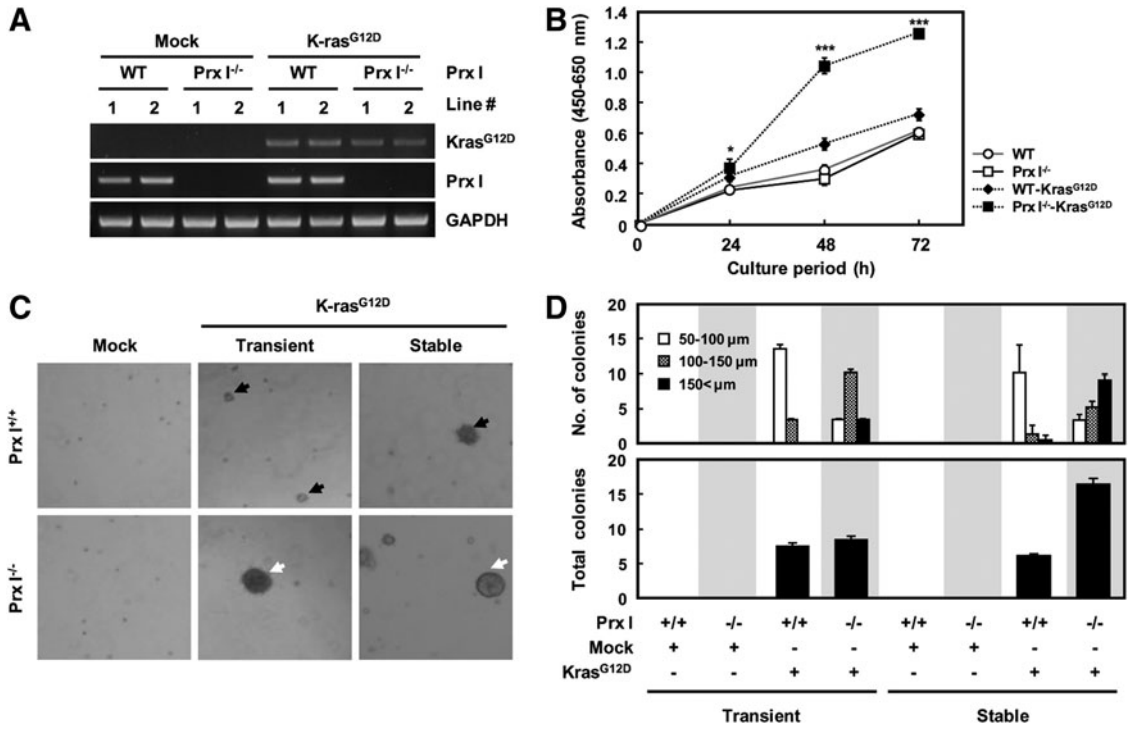

FIG. 4. Deficiency of Prx I impaired cell proliferation and anchorage-independent growth. (A) Generation of stable cell lines expressing K-ras^{G12D} in WT and Prx I$^{-/-}$ 3T3-MEFs. **(B)** Cellular proliferation effects of K-ras^{G12D} 3T3-MEFs with Prx I inactivation were measured by CCK-8 assay at the indicated time. The data are representative of at least three different experiments and presented as mean ± SEM. $^{*}p < 0.05$, $^{***}p < 0.001$ compared with WT-K-ras^{G12D} 3T3-MEFs. **(C)** Anchorage-independent growth assay was performed in 3T3-MEFs transfected with transiently or stably expressing K-ras^{G12D}. The diameters of the colonies were indicated by *black* (100–150 μm) or *white* (>150 μm) *arrows*. **(D)** The number of colonies was determined by counting duplicated plates. The diameters of the colonies were 50–100 μm, 100–150 μm, and >150 μm. CCK-8, cell counting kit-8; MEFs, mouse embryonic fibroblasts.

ROS-produced nearby growth factor receptors, leading to modulation of protein tyrosine phosphatase (PTP) activity (42). Conversely, PTPs also regulate Prx activity by reducing its phosphorylation. It is suggestive of the precise role of ROS as second-messenger-governing Prx-PTP network. Importantly, PTPs are generally known to be involved in a variety of pathological conditions, including diabetes mellitus, neural diseases, allergy, and inflammation (20). Moreover, PTPs are considered promising cancer therapeutic targets (20). Based on the close relationship between Prxs and PTPs, therefore, many researchers have attempted to profile Prx isotypes using a variety of human cancer tissues to define major regulators of tumorigenesis as well as potential prognostic biomarkers. Although aberrant expression of Prx members is frequently found in lung tumor regions, the expression profiles are quite different between studies (31, 44, 52, 60). In particular, however, Prx I appears to be constantly up-regulated in lung tumors compared with the other members (9, 27, 28). In the current study, we have also investigated the expression levels of Prx isotypes using human adenocarcinoma samples and numerous lung cell lines, including adenocarcinoma and nontransformed cells. Prxs III, V, and VI were unaltered in protein levels between normal and tumor regions; whereas Prx II was greatly decreased in tumor regions compared with normal tissues (Supplementary Fig. S6A, B). In contrast, Prx I and Prx IV were significantly up-regulated in the tumor region (Supplementary Fig. S6A, B). Similarly, Prx I and Prx IV were also increased in adenocarcinoma cell lines compared with nontransformed Beas2B cells (Supplementary Fig. S6C). To define the intracellular redox signaling pathways governed by Prx during lung tumorigenesis, we excluded secretory antioxidant Prx IV because of its extracellular residence and studies concerning Prx I. In addition, other antioxidants such as glutathione peroxidases (GPx) 1 and catalase were significantly decreased in tumor regions compared with nontumor tissues (data not shown). Thus, we propose that Prx I may be a major player in ROS-mediated lung tumorigenesis as well as a potential prognostic marker for lung adenocarcinoma.

Prx I has two conflicting roles regarding tumorigenesis. Knockout-mouse studies have shown that Prx I is a tumor suppressant (7, 15, 41), whereas many other studies have also revealed that the presence of Prx I in a tumor contributes to tumor protection or maintenance (10, 45). These demonstrations indicate that Prx I plays different roles depending on tumor stages. However, Prx I functions as a tumor suppressant in lung adenocarcinogenesis of K-ras^{G12D}-Tg mice as well as in A549 cells overexpressed with human Prx I. Consistent with other studies using Prx I-null mice (41), the present study also showed that tumor formation was detected only in Prx I$^{-/-}$ mice, mainly in lung tissue, and that ~25% of Prx I$^{-/-}$ mice developed lung cancer from 12 months of age (Supplementary Table S1). Although extensive tumor formation and metastasis were not found in the lungs of Prx I$^{-/-}$ mice, as shown in the study by Neumann and colleagues (40, 41), the current data suggest that the

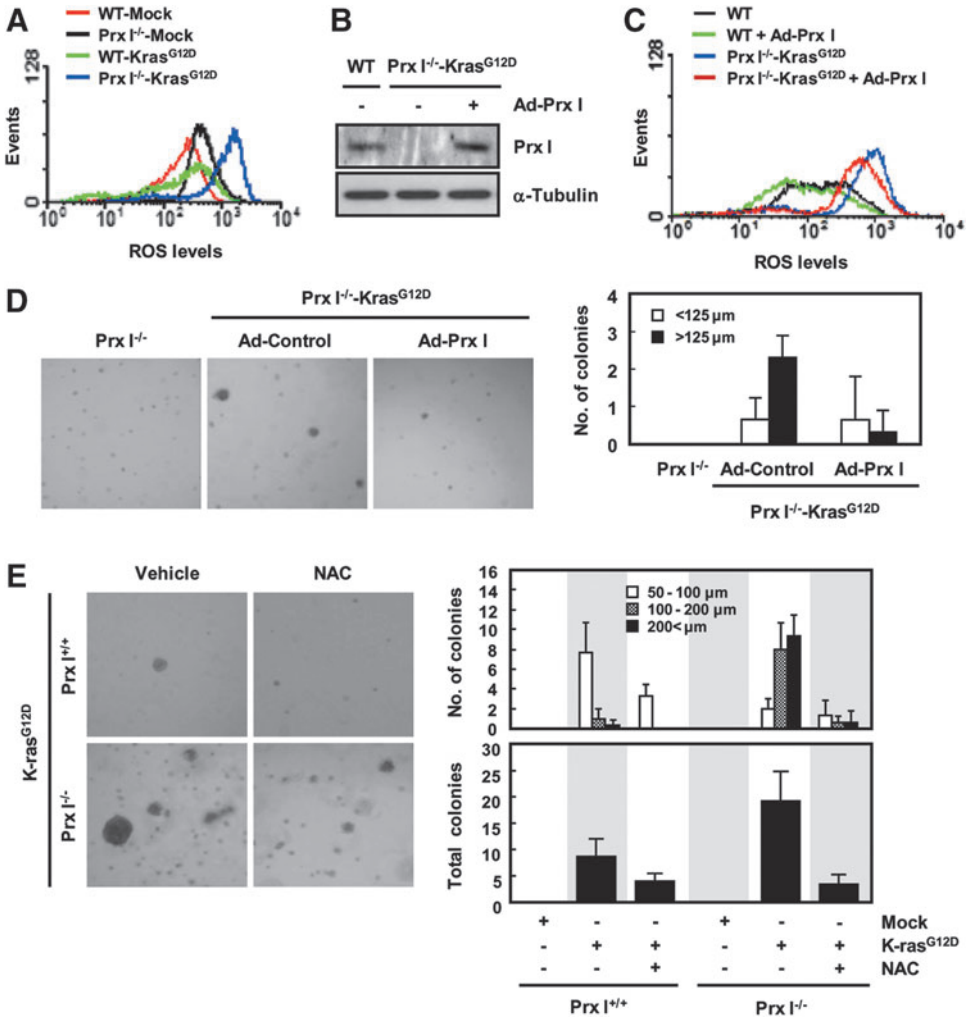

FIG. 5. Prx I regulates K-ras^{G12D}-induced intracellular ROS production. (A) WT and Prx I$^{-/-}$ 3T3-MEFs were stably transfected with the K-ras^{G12D} gene and incubated with CM-H_2DCFDA. ROS generation was determined by flow cytometry. The data are representative of at least three different experiments. **(B)** Western blot for Prx I protein levels in K-ras^{G12D}/Prx I$^{-/-}$ 3T3-MEFs infected with Ad-Prx I. **(C)** ROS levels were detected in the K-ras^{G12D}/Prx I$^{-/-}$ 3T3-MEFs infected with the control virus (Ad-Control and Ad-Prx I). The data are representative of at least three different experiments. **(D)** Microscopic appearance and quantification of anchorage-independent growth in the K-ras^{G12D}/Prx I$^{-/-}$ 3T3-MEFs infected with Ad-Prx I. The diameters of the colonies were < 125 μm and > 125 μm. The number of colonies was determined by counting duplicated plates. **(E)** Microscopic appearance and quantification of anchorage-independent growth in the MEFs with N-acetyl L-cysteine (NAC) treatment compared with the vehicle-treated MEFs. The diameters of the colonies were 50–100 μm, 100–200 μm, and > 200 μm. The number of colonies was determined by counting duplicated plates. ROS, reactive oxygen species. To see this illustration in color, the reader is referred to the web version of this article at www.liebertpub.com/ars

primary role of Prx I is closely associated with tumor suppression.

Augmented Prx I content is frequently found in a variety of malignant tumors. Nevertheless, increased intracellular ROS levels are also found in tumor cells, indicating that basal redox level is maintained at a higher level in cancer cells compared with normal cells. Thus, many redox-sensitive pathways may be activated during tumorigenesis (58). In the current study, Nrf2 was increased in human lung adenocarcinoma and K-ras^{G12D}-transformed tissues; whereas Keap1 content was greatly reduced, resulting in augmented expression of the target genes, such as Prx I and HO-1. In agreement with other reports (14, 43), the Nrf2 expression level was highly dependent on ROS level, which was indicative of a high Nrf2/Keap1 ratio as a redox-sensitive pathway or a possible prognostic marker in NSCLC. Interestingly, we further found that the Nrf2/keap1 ratio was inversely associated with Prx I content, which is highly dependent on redox status (Fig. 10), suggesting a cooperative connection between Prx I/ROS and Nrf2 pathways. Consistent with data from mouse-lung tissue, high Nrf2/Keap1 ratio and HO-1 up-regulation were found in Prx I$^{-/-}$ 3T3-MEFs, siPrx I-transfected A549 cells, and NCI-H358 cells compared with the corresponding control cells (Fig. 10A–C). Conversely, overexpression of Prx I in A549 cells suppressed the expression of Nrf2 and HO-1 compared with control cells (Fig. 10D). These results suggest that a novel feedback mechanism in expression between Nrf2 and Prx I may be present in lung tissues.

The role of Nrf2 in lung cancer is directly correlated with cell proliferation (22). Consistent with this, our data also

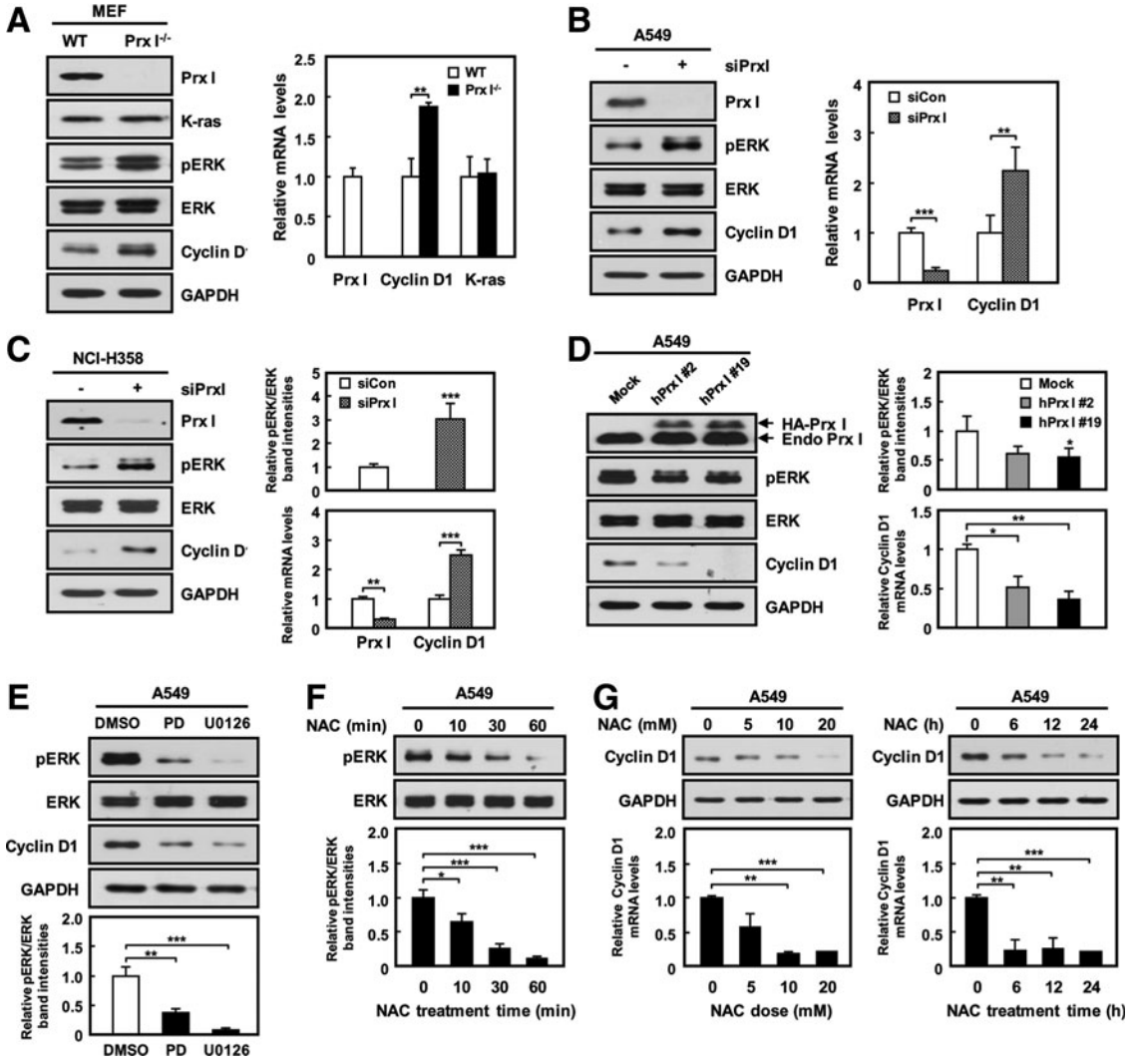

FIG. 6. Prx I regulates ERK/cyclin D1 pathway in cell proliferation. (A) Cell extracts from 3T3-MEFs were measured with antibodies that were specific for Prx I, K-ras, pERK, and cyclin D1. ERK and GAPDH were used as loading controls. Expression levels of Prx I, cyclin D1, and K-ras mRNA in WT and Prx $I^{-/-}$ 3T3-MEFs were analyzed by qPCR. The data are representative of at least three different experiments and presented as mean ± SEM. $^{**}p < 0.01$ compared with WT 3T3-MEFs. **(B)** Western blots and qPCR for Prx I, pERK, and cyclin D1 in siPrx I-transfected A549 cells. The data are representative of at least three different experiments and presented as mean ± SEM. $^{**}p < 0.01$, $^{***}p < 0.001$ compared with the cells transfected with scrambled siRNA. **(C)** Western blots and qPCR for Prx I, pERK, and cyclin D1 in siPrx I-transfected NCI-H358 cells. The data are representative of at least three different experiments and presented as mean ± SEM. $^{**}p < 0.01$, $^{***}p < 0.001$ compared with the cells transfected with scrambled siRNA. **(D)** Western blot and qPCR analysis for pERK and cyclin D1 in A549 cells stably transfected with mock or HA-Prx I expression vectors. The data are representative of at least three different experiments and presented as mean ± SEM. $^{*}p < 0.05$, $^{**}p < 0.01$ compared with A549 Mock cells. **(E)** Western blot analysis against pERK and cyclin D1 in A549 cells were treated with ERK inhibitors (PD98059; 20 μM or U0126; 10 μM) for 24 h. DMSO only was administered as the control treatment. The data are representative of at least three different experiments and presented as mean ± SEM. $^{**}p < 0.01$, $^{***}p < 0.001$ compared with untreated cells. **(F)** Western blots for ERK and pERK in A549 cells treated with 10-mM NAC for 0, 10, 30, and 60 min. The data are representative of at least three different experiments and presented as mean ± SEM. $^{*}p < 0.05$, $^{***}p < 0.001$ compared with untreated cells. **(G)** Cyclin D1 protein and mRNA levels in A549 cells treated with 0, 5, 10, and 20 mM NAC for 24 h. or 20 mM NAC for 0, 6, 12, and 24 h. The data are representative of at least three different experiments and presented as mean ± SEM. $^{**}p < 0.01$, $^{***}p < 0.001$ compared with untreated cells. DMSO, dimethyl sulfoxide; ERK, extracellular signal-regulated kinase.

include both activation of the Nrf2 pathway and enhancement of cell proliferation in K-ras^{G12D} cells and mice. Most of all, Nrf2 pathway and cyclin D1 expression were notably increased in Prx $I^{-/-}$/K-ras^{G12D}-Tg lung tissue compared with any other genotypes (Figs. 3F and 8A–C), which is in good accord with the degree of tumor progression. In addition, recent studies have revealed that oncogenic transformation requires the activation of an ROS-dependent signal pathway to enhance proliferation and subsequent tumor progression (57). Moreover, siNrf2 transfection led to activation of the ERK/cyclin D1 pathway in A549 cells, which seemed to be related to the increase in ROS by reduction of the Prx I level (Fig. 10F). Based on these findings, we propose that K-ras-mediated tumor growth may be dependent on cooperative

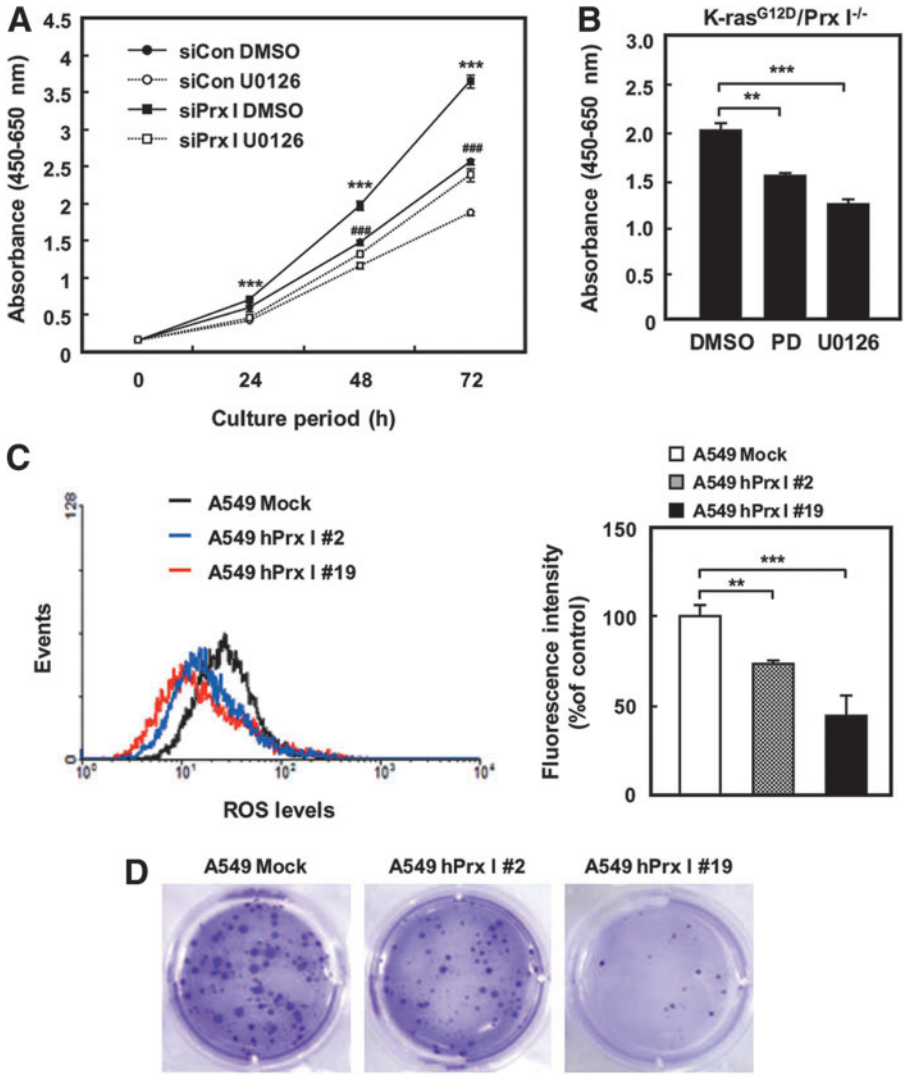

FIG. 7. ROS/ERK pathway involves oncogenic K-ras-driven tumor growth. (A) NCI-H358 cells were transfected with siPrx I and cultured in the presence or absence of U0126 (10 μM) and subjected to CCK-8 cell proliferation assay at the indicated time. The data are representative of at least three different experiments and presented as mean ± SEM. $^{***}p < 0.001$ compared with the cells transfected with siPrx I cultured in U0126, $^{***}p < 0.001$ compared with the cells transfected with scrambled siRNA cultured in U0126. **(B)** CCK-8 cell proliferation assay was carried out using K-ras^{G12D}/Prx I$^{-/-}$ 3T3-MEFs cells cultured in the presence or absence of U0126 (10 μM) or PD98059 (20 μM) for 72 h. The data are representative of at least three different experiments and presented as mean ± SEM. $^{**}p < 0.01$, $^{***}p < 0.001$ compared with the cells cultured in DMSO. **(C)** A549 cells were stably transfected with human Prx I expression vector, and ROS levels were measured by flow cytometry. The data are representative of at least three different experiments and presented as mean ± SEM. $^{**}p < 0.01$, $^{***}p < 0.001$ compared with A549 Mock cells. **(D)** Anchorage-independent growth assay was performed using stably expressed Prx I in A549 cells. The data are representative of at least three different experiments. To see this illustration in color, the reader is referred to the web version of this article at www.liebertpub.com/ars

redox regulation among ROS, Nrf2, and Prx I, and that the chain reaction among them may ultimately contribute to accumulation of high levels of ROS in cancer.

The ERK pathway is reported to be a critical signaling cascade in oncogenic mutation-associated tumorigenesis (35, 55). Actually, aberrant activation of K-ras ultimately leads to oncogenic transformation in numerous cancers by enhancing the ERK pathway (47). Notably, ERK is well known for governing oncogenic K-ras-driven lung tumor physiology, such as cell proliferation and survival (56). Thus, it is important to find a key modulator of the oncogenic K-ras/ERK pathway for the improvement of therapeutic modality in NSCLC. Consistent with these demonstrations, our data also showed that K-ras-driven lung tumorigenesis is dependent on the activation of the ERK pathway. ERK-dependent tumor growth appeared to be closely associated with cyclin D1 expression (3, 37). In 2009, Cao and colleagues have revealed that Prx I deficiency accelerates Ras-induced tumorigenesis in mammary glands through modulation of PTEN/AKT signaling pathway (7). They also demonstrated that Prx I physiologically interacts with PTEN to protect oxidative inactivation, providing a mechanism of Prx I-mediated tumor suppression. Similar to ERK, NF-κB, JAK/STAT, and Wnt/β-catenin (32), PTEN/AKT pathway is also known as an inducer of cyclin D1 gene transcription, but the involvement of cyclin D1 in the acceleration of Ras-induced tumorigenesis by Prx I deficiency is not addressed (7). In contrast, we first assessed the participation of ERK/cyclin D1 axis in Prx I-deficiency-mediated lung tumorigenesis. Taken together, we have demonstrated that the up-regulation of Prx I actively participates in the suppression of the K-ras/ERK/cyclin D1 cascade during lung tumorigenesis and that the antitumor activity of Prx I requires redox-sensitive Nrf2 pathway activation. Collectively, these observations led us to suggest the role of Prx I and its underlying mechanism in oncogenic K-ras-driven tumorigenesis (Fig. 8D) and to conclude that Prx I acts as an Nrf2-dependent, inducible tumor suppressant by opposing the K-ras/ERK/cyclin D1 pathway in NSCLC. Currently, we are trying to define the precise role of Prx I in regulation of the ERK pathway in NSCLC by screening physically interacting molecules.

In summary, the current study suggested that an enhanced Prx I level contributes to the inhibition of K-ras-driven lung tumorigenesis. Prx I was significantly up-regulated in the tumor regions *via* activation of the Nrf2 transcription factor, and an increase in the ROS level by null mutation of Prx I severely aggravated K-ras-driven lung tumorigenesis *via* the activation of the redox-sensitive ERK/cyclin D1 pathway.

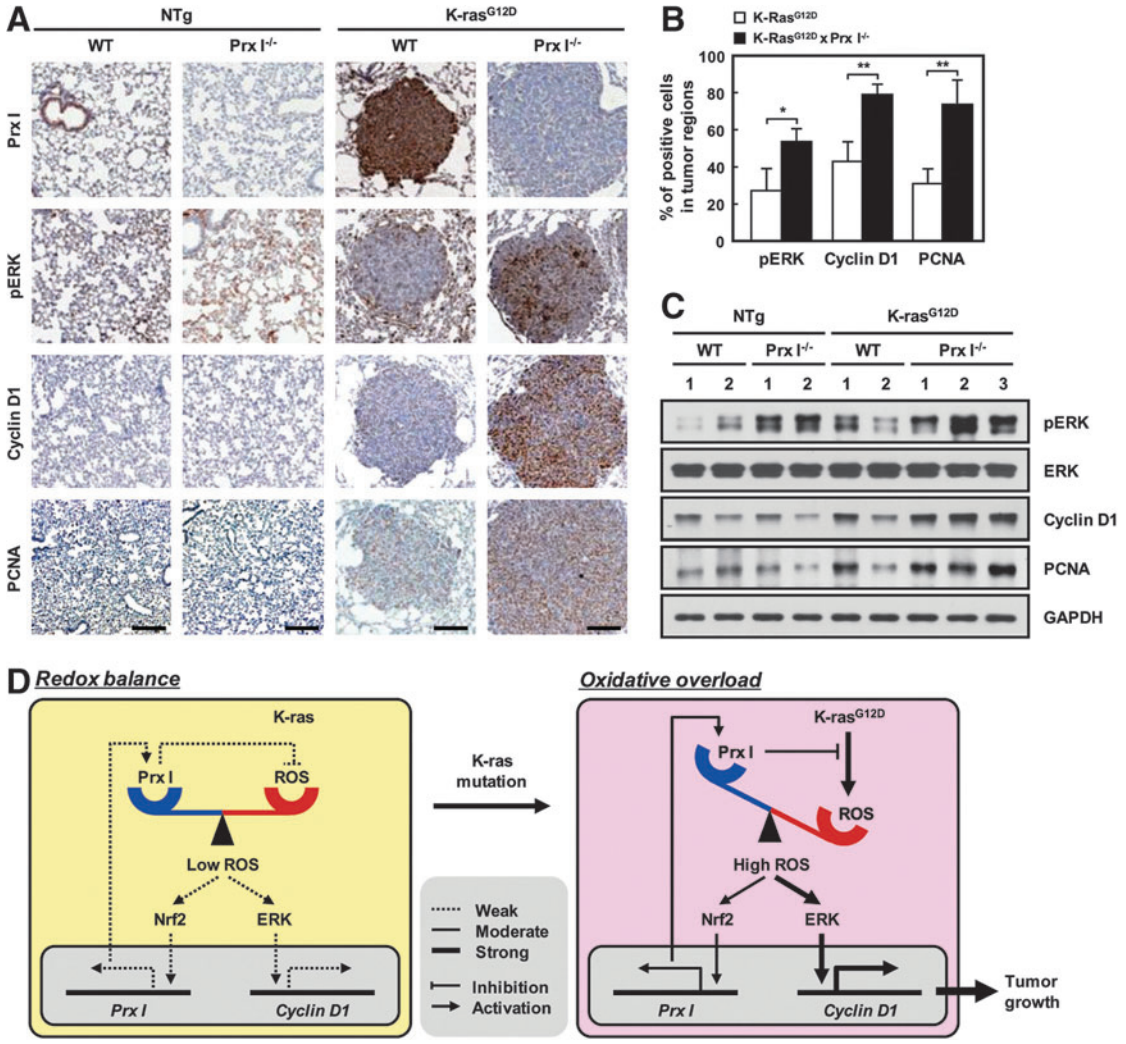

FIG. 8. Prx I inactivation promotes lung tumor growth in K-ras^{G12D}-Tg mice. (A) Immunostaining of Prx I, pEKR, cyclin D1, and PCNA in lungs from four groups of mice at 7 months (Scale bars, 50 μm). **(B)** Quantitation of pERK, cyclin D1, and PCNA-positive cells per tumor area at five different time points at 7 months. The data are presented as the mean ± SEM ($n = 5$). $^{*}p < 0.05$, $^{**}p < 0.01$ compared with WT/K-ras^{G12D}-Tg mice. **(C)** Western blots for pERK, cyclin D1, and PCNA in lungs from WT ($n = 2$), Prx I$^{-/-}$ ($n = 2$), WT/K-ras^{G12D}-Tg ($n = 2$), and Prx I$^{-/-}$/K-ras^{G12D}-Tg ($n = 3$) mice at 7 months. **(D)** Schematic illustration of the expression and function of Prx I in K-ras^{G12D}-driven lung adenocarcinoma. To see this illustration in color, the reader is referred to the web version of this article at www.liebertpub.com/ars

Collectively, these results suggest that Prx I functions as an Nrf2-dependent, inducible tumor suppressant in K-ras^{G12D}-driven lung adenocarcinogenesis by opposing ROS/ERK/cyclin D1 pathway activation. These findings provide a better understanding of oxidative stress-mediated lung tumorigenesis and therapeutic modality for oncogenic K-ras-associated NSCLC patients. Prx I has become an important target molecule for managing lung cancers, offering a new direction for therapeutic approaches.

Materials and Methods

Animal models

The K-ras^{G12D}-Tg mouse was generated in which the expression of the mutated mouse K-ras^{G12D} is targeted to lung alveolar type II cells by human surfactant protein-c 3.7 kb promoter. A 608 bp fragment of mouse K-ras^{G12D} was isolated *via* PCR from mouse cDNA, and site-directed mutagenesis was done by overlapping extension. PCR using the sense primer 1: 5′-CGGAGAGAGGCCTGCTGA-3′ antisense 1: 5′-CTTGCCTACGCCA**T**CAGCT-3′, sense primer 2: 5′-AG CTG**A**TGGCGTAGG**C**AAG-3′, antisense 2: 5′-ATGGTCCG GAAGCTTCATTATC-3′ primer pairs and PrimeSTAR™ HS DNA polymerase with proofreading capability (Takara). Bolded and underlined characters indicate a point mutation at codon 12 of the K-ras gene. The PCR product was digested with *Eco*RI and subcloned into the pBluescript2 SK(−) vector (Supplementary Fig. S7). The constructs were verified by DNA sequencing in both directions. The insert DNA was released from the pBluescript2 SK(−) vector by *Sal*I/*Not*I digestion, purified, and diluted to a final concentration of 4 ng/μl for the pronuclear injection. Prx I$^{-/-}$/K-ras^{G12D}-Tg (double mutant) mice were produced by crossing K-ras^{G12D}-Tg mice with Prx I$^{-/-}$ mice. The genotyping primers for K-ras^{G12D} were 5′-CAGGAACAAACAGGCTTCAAA-3′ and 5′-TTATGGCAAATACACAAAG AAAGC-3′. The genotyping

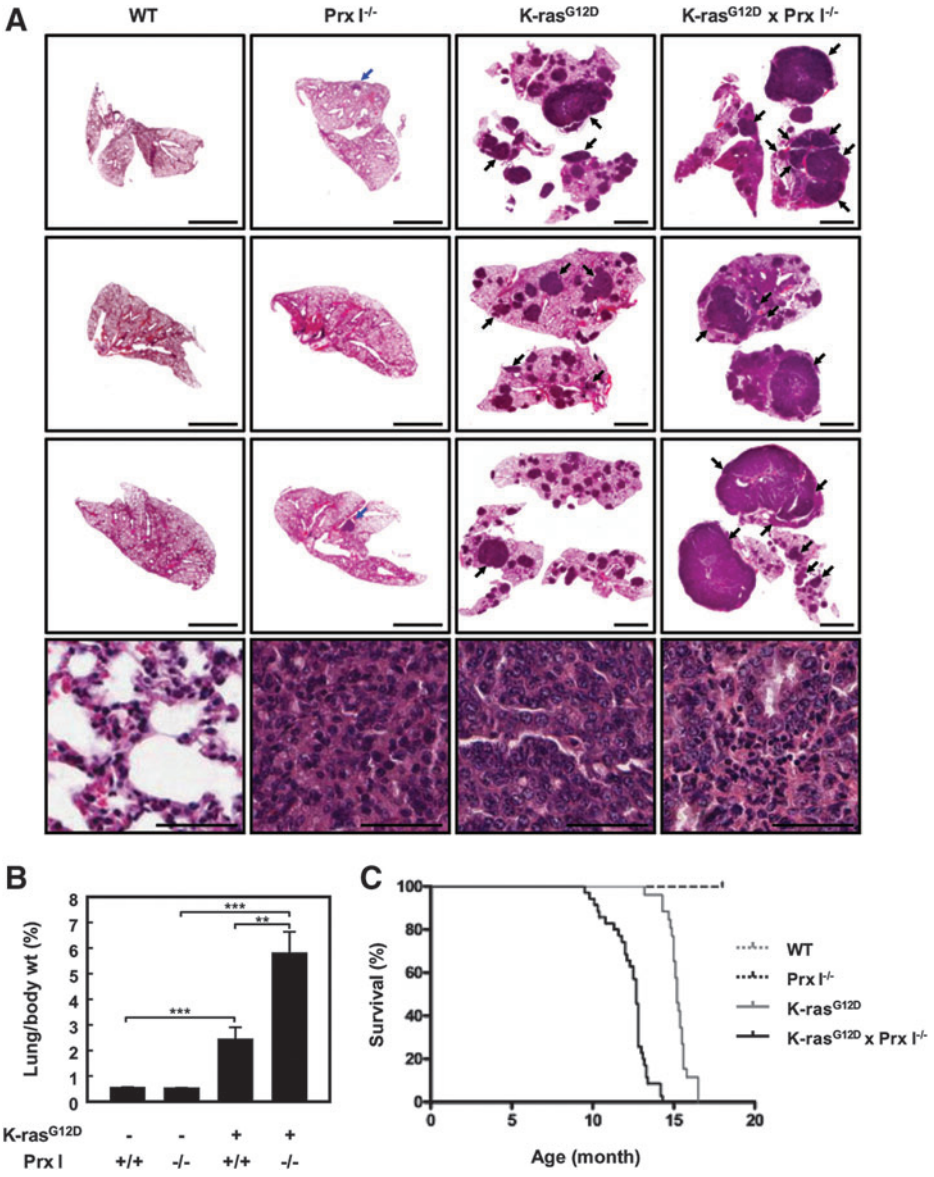

FIG. 9. Prx I deficiency accelerates K-ras^{G12D}-driven lung adenocarcinoma in mice. (A) Three independent mice with the indicated genotype were sacrificed at 12 months and subjected to H&E staining (Scale bars, 4 mm). Adenoma is indicated by *blue arrows* in Prx I$^{-/-}$ mice, adenocarcinomas are indicated by *black arrows*, and high magnification images are shown in the *bottom panel* (Scale bars, 50 μm). **(B)** Measurement of lung weight using 12-month-old mice with the indicated genotypes (WT; $n=11$, Prx I$^{-/-}$; $n=11$, WT/K-ras^{G12D}-Tg; $n=8$, Prx I$^{-/-}$/K-ras^{G12D}-Tg; $n=7$). The data are presented as the mean ± SEM. $^{**}p<0.01$, $^{***}p<0.001$. **(C)** Age-dependent survival curves of the mice with indicated genotype. (WT; $n=20$, Prx I$^{-/-}$; $n=20$, WT/K-ras^{G12D}-Tg; $n=35$, and Prx I$^{-/-}$/K-ras^{G12D}-Tg; $n=26$ for survival analysis). Median survival values of WT/K-ras^{G12D}-Tg and Prx I$^{-/-}$/K-ras^{G12D}-Tg mice were 15.2 and 12.7 months, respectively. $p<0.0001$ (log-rank test for WT/K-ras^{G12D}-Tg *versus* Prx I$^{-/-}$/K-ras^{G12D}-Tg). To see this illustration in color, the reader is referred to the web version of this article at www.liebertpub.com/ars

primers for Prx I were 5′-CTGGAAACCTGGCAGTGATA-3′ and 5′-CTGTGACTGATAGAAGATTGGT-3′. All animal procedures were conducted in accordance with the guidelines of the Institutional Animal Care and Use Committee, Korea Research Institute of Bioscience and Biotechnology.

Cell culture and treatments

WT and Prx I$^{-/-}$ mouse embryonic fibroblasts (MEFs) were isolated from fetuses of 13.5 days postcoitum and cultured in Dulbecco's modified Eagle's medium (DMEM; Invitrogen) containing 10% fetal bovine serum (FBS; HyClone) and antibiotics. To establish immortalized cell lines, WT and Prx I$^{-/-}$ MEFs were passaged 50 times every 3 to 5 days by trypsinization with 0.25% trypsin/5.3 m*M* EDTA, which was called MEF-derived NIH3T3-like cells (3T3-MEFs). Human lung cancer cell lines A549 and NCI-H358 were propagated in Ham's F12K medium (Invitrogen) and RPMI 1640 medium containing 10% FBS and antibiotics. The MEK1/2 inhibitors PD98059 (Calbiochem; 18.7 m*M*) and U0126 (Cell Signaling Technology; 10 m*M*) were dissolved in dimethyl sulfoxide. Cells were stimulated and cultured in a medium that always contained PD98059, U0126, or an equivalent volume of DMSO carrier.

Plasmid construction and transfection

The pCAGGS-K-ras^{G12D}-puro and pCAGGS-hPrx I-HA-neo vector was constructed as follows. The coding sequences for mutated K-ras (K-ras^{G12D}) and human Prx I (hPrx I) were inserted by PCR cloning into the *Eco*RI site of the pCAGGS-puro and pCAGGS-HA-neo vector and confirmed by restriction mapping and DNA sequencing. A549, WT 3T3-MEFs, and Prx I$^{-/-}$ 3T3-MEFs were plated in six-well culture plates and transfected with 3 μg of pCAGGS-hPrx I-HA-neo and pCAGGS-K-ras^{G12D}-puro constructs using a Lipofectamine 2000 reagent (Invitrogen) according to the manufacturer's instructions. After 48 h, cells were trypsinized and plated in a medium containing 1 μg/ml puromycin or 400 μg/ml neomycin (Invitrogen). After selection for 2 weeks, the colonies were isolated and propagated into 96-well plates with a growth medium containing 1 μg/ml puromycin or 400 μg/ml

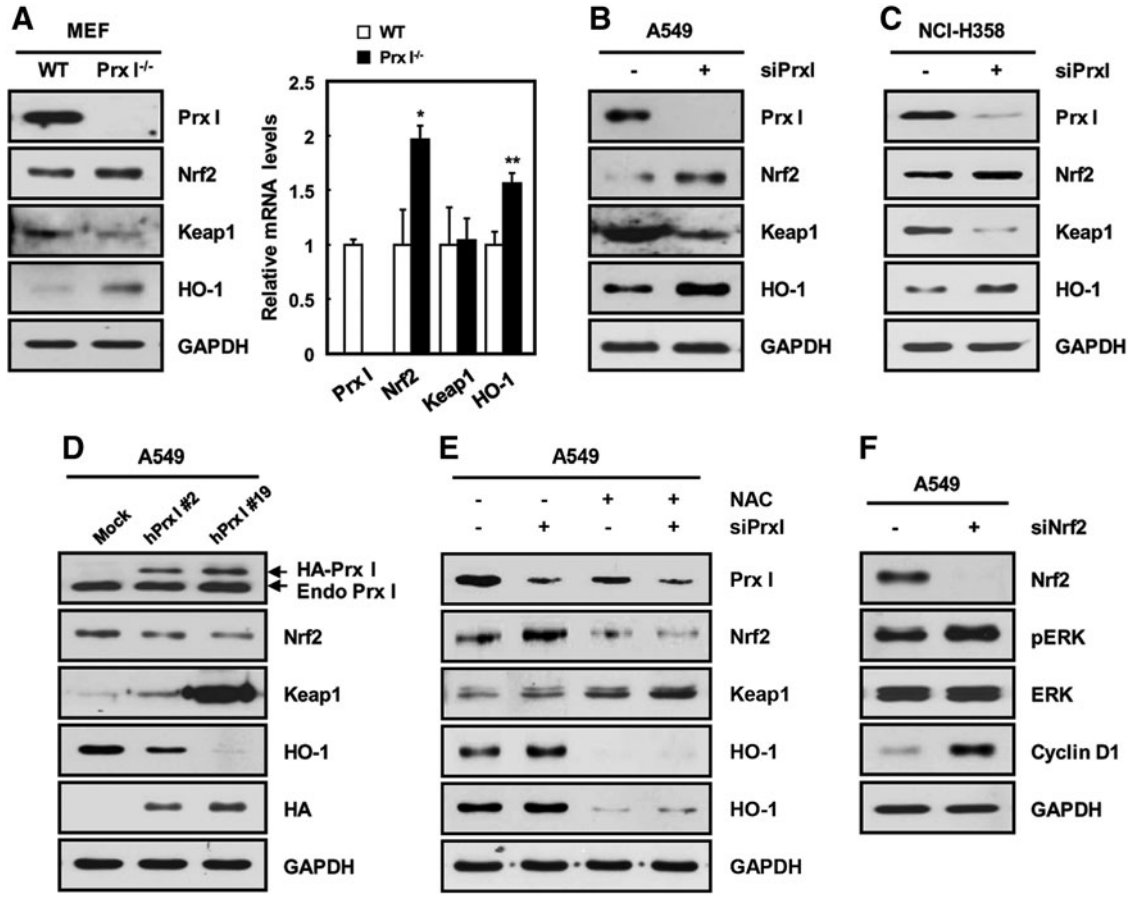

FIG. 10. ROS-dependent reciprocal regulation between Prx I and Nrf2. (A) Prx I deficiency caused increased expression levels of Nrf2 and HO-1 and a decrease in Keap1 in 3T3-MEFs. The data are representative of at least three different experiments and presented as mean ± SEM. $^{*}p < 0.05$, $^{**}p < 0.01$ compared with WT 3T3-MEFs. **(B, C)** Effect of Prx I knockdown on Nrf2, keap1, and HO-1 protein levels in A549 **(B)** and NCI-H358 cells **(C)**. **(D)** A549 cells were stably transfected with human Prx I vectors and cell lysates derived from two established independent stable clones (#2 and #19); they were subjected to immunoblotting with anti-Prx I, Nrf2, Keap1, and HO-1. Immunoblotting with an anti-HA antibody showed exogenously overexpressed Prx I. **(E)** Effect of combined treatment with siPrx I and NAC on protein levels of Nrf2, Keap1, and HO-1 in A549 cells. **(F)** A549 cells were transfected with siNrf2 and subjected to Western blotting analysis against Nrf2, pERK, ERK, and cyclin D1. The data are representative of at least three different experiments.

neomycin. For determination of transformants, the cell clones were subjected to both Western blot analysis using K-ras (Santa Cruz Biotechnology) or HA (Roche) antibodies and RT-PCR analysis using K-ras detection primers.

Quantitative real-time PCR analysis

Total RNA was prepared from cells or human tissues using TRIzol (Molecular Research Center) according to the manufacturer's protocol. cDNA synthesized with oligo (dT) primers with the first-strand cDNA Synthesis kit (Fermentas) was mixed with the SYBR Premix Ex Taq (Takara) and sets of gene-specific primers. Sequences for the primers used for this study are provided in Supplementary Table S2.

Western blot analysis

We homogenized lung tissues and cell lysates in a lysis buffer (20-m*M* HEPES, 150-m*M* NaCl, 2-m*M* EGTA, 1-m*M* EDTA, 20-m*M* glycerol phosphate, 1% Triton X-100, and 10% glycerol) with protease (Sigma) and a phosphatase-inhibitor cocktail (Roche). Proteins were separated by SDS-PAGE, transferred to nitrocellulose membranes (Millipore), and identified by immunoblotting. The membranes were primarily blotted with primary antibodies against Prx I, GAPDH (both from ABfrontier), ERK, cyclin D1, HO-1, pERK (four from Cell Signaling Technology), Nrf2, Keap1, K-ras (three from Santa Cruz Biotechnology), PCNA (DakoCytomation), and α-Tubulin (Sigma) at 4°C overnight. The membranes were washed five times with 10-m*M* Tris-HCl (pH 7.5) containing 150-m*M* NaCl and 0.2% Tween-20 (TBST) and incubated with horseradish peroxidase-conjugated goat anti-rabbit IgG or anti-mouse IgG (both from Sigma) for 1 h at 25°C. After the removal of excess antibodies by washing with TBST, specific binding was detected using a SuperSignal chemiluminescent substrate (Pierce) according to the manufacturer's instructions.

Measurement of intracellular ROS

Intracellular ROS generation was assessed with a 5,6-chloromethyl-2′,7′-dichlorodihydrofluorescein diacetate

(CM-H_2DCFDA; Invitrogen), an ROS indicator. Exponentially growing MEFs were incubated with 5 μM CM-H2DCFDA at 37°C for 5 min and washed twice with PBS by centrifugation at 200 *g* for 5 min. The cells were resuspended with PBS and analyzed by flow cytometry on an FACSCalibur instrument (BD Biosciences).

Colony-formation assay in soft agar

MEFs ($0.4–1.6 \times 10^5$ cells) were suspended in 1 ml of DMEM containing 0.3% agar in cell-growth medium and plated in triplicates over a first layer of 0.6% agar in growth medium. The cells were grown at 37°C and 5% CO_2, and colonies were counted at day 14 and day 21. Colonies of eight cells or more were counted and photographed with 30 fields in each plate, and results were graphed from two independent experiments. Then, viable colonies were stained with 0.01% crystal violet (Sigma) for 10 min. We treated the cells requiring 10-m*M* NAC (Sigma) treatment with NAC in the top agar on day 0. The NAC-containing medium was replaced over agar every day. Assays were done in triplicate and in all cases, independently, at least twice.

Cell-proliferation assay

Cells were seeded at a density of 1000 cell/well into 96-well cell culture plates. Cells were grown for 72 h. Cell counting kit-8 (CCK-8; Dojindo) solution was added to each well. After 1 h, the absorbance at 450 nm of each well was read on a microplate reader (VERSAmax™).

Immunohistochemistry

Lung tissues were fixed overnight with 10% neutral-buffered formalin, embedded in paraffin, and processed for sections of 4 μm thicknesses. Additional details were performed as previously described (53).

Transfection of small interfering RNA

Approximately 3×10^5 cells were seeded on 60 mm culture dishes and transfected with small interfering RNAs using Lipofectamine RNAi Max (Invitrogen) according to the manufacturer's instructions. Target sequences for knockdown of human Prx I were #1 5′-AAACUCAACUGCCAAGUGA-3′, #2 5′-CCACGGAGAUCAUUGCUUU-3′, #3 5′-GCAGA AGAAUUUAAGA AAC-3′, Nrf2 and K-ras siRNA (Dharmacon), and Scramble siRNA 5′-UUCUUCGAACGUGU GUCACGUUU-3′. Prx I, Nrf2, and K-ras mRNA and protein levels were evaluated by both RT-PCR (48 h post-transfection) and immunoblotting assays (72 h posttransfection), correspondingly.

Patient tissue samples

Pairs of primary lung adenocarcinoma and adjacent nontumourous lung parenchyma tissues were collected from patients ($n = 21$) undergoing lung cancer resection surgery at the Korea University of Medicine in Seoul, Korea. All study patients provided informed consent before surgery.

Statistical analysis

Data were analyzed using a Student's *t*-test on SigmaPlot 12.3 software, and the *p*-value was derived to assess statistical significance. Error bars correspond to SEM. Survival data were analyzed with the Gehan–Breslow–Wilcoxon test by using Prism software. A *p*-value of less than 0.05 was considered significant.

Acknowledgments

The authors thank Sang Won Kang for providing Ad-Prx I; Sang-Mi Cho and Mi-Ra Jung of the authors' laboratory for technical assistance and animal care. This work was supported by the World Class Institute (WCI) Program of the National Research Foundation of Korea (NRF); funded by the Ministry of Education, Science, and Technology of Korea (MEST) (NRF Grant Number: WCI 2009-002), by the Research Program for New Drug Target Discovery Grant (NBM3300711) from the Ministry of Education, Science, and Technology, by the National Foundation of Korea (NRF) Grant funded by the Korea Government (OGM0021211), and by the KRIBB Research Initiative Program Grant (KGM3320911).

Author Disclosure Statement

No competing financial interests exist.

References

1. Abbas K, Breton J, Planson AG, Bouton C, Bignon J, Seguin C, Riquier S, Toledano MB, and Drapier JC. Nitric oxide activates an Nrf2/sulfiredoxin antioxidant pathway in macrophages. *Free Radic Biol Med* 51: 107–114, 2011.
2. Alexandrova AY, Kopnin PB, Vasiliev JM, and Kopnin BP. ROS up-regulation mediates Ras-induced changes of cell morphology and motility. *Exp Cell Res* 312: 2066–2073, 2006.
3. Arber N, Sutter T, Miyake M, Kahn SM, Venkatraj VS, Sobrino A, Warburton D, Holt PR, and Weinstein IB. Increased expression of cyclin D1 and the Rb tumor suppressor gene in c-K-ras transformed rat enterocytes. *Oncogene* 12: 1903–1908, 1996.
4. Avila PC, Kropotov AV, Krutilina R, Krasnodembskay A, Tomilin NV, and Serikov VB. Peroxiredoxin V contributes to antioxidant defense of lung epithelial cells. *Lung* 186: 103–114, 2008.
5. Bae SH, Sung SH, Cho EJ, Lee SK, Lee HE, Woo HA, Yu DY, Kil IS, and Rhee SG. Concerted action of sulfiredoxin and peroxiredoxin I protects against alcohol-induced oxidative injury in mouse liver. *Hepatology* 53: 945–953, 2011.
6. Butterfield LH, Merino A, Golub SH, and Shau H. From cytoprotection to tumor suppression: the multifactorial role of peroxiredoxins. *Antioxid Redox Signal* 1: 385–402, 1999.
7. Cao J, Schulte J, Knight A, Leslie NR, Zagozdzon A, Bronson R, Manevich Y, Beeson C, and Neumann CA. Prdx1 inhibits tumorigenesis via regulating PTEN/AKT activity. *EMBO J* 28: 1505–1517, 2009.
8. Chang F, Steelman LS, Shelton JG, Lee JT, Navolanic PM, Blalock WL, Franklin R, and McCubrey JA. Regulation of cell cycle progression and apoptosis by the Ras/Raf/MEK/ERK pathway (Review). *Int J Oncol* 22: 469–480, 2003.
9. Chang JW, Jeon HB, Lee JH, Yoo JS, Chun JS, Kim JH, and Yoo YJ. Augmented expression of peroxiredoxin I in lung cancer. *Biochem Biophys Res Commun* 289: 507–512, 2001.
10. Chen MF, Keng PC, Shau H, Wu CT, Hu YC, Liao SK, and Chen WC. Inhibition of lung tumor growth and augmentation of radiosensitivity by decreasing peroxiredoxin I expression. *Int J Radiat Oncol Biol Phys* 64: 581–591, 2006.

11. Choi MH, Lee IK, Kim GW, Kim BU, Han YH, Yu DY, Park HS, Kim KY, Lee JS, Choi C, Bae YS, Lee BI, Rhee SG, and Kang SW. Regulation of PDGF signalling and vascular remodelling by peroxiredoxin II. *Nature* 435: 347–353, 2005.
12. Coleman ML, Marshall CJ, and Olson MF. Ras promotes p21(Waf1/Cip1) protein stability via a cyclin D1-imposed block in proteasome-mediated degradation. *EMBO J* 22: 2036–2046, 2003.
13. Collins LG, Haines C, Perkel R, and Enck RE. Lung cancer: diagnosis and management. *Am Fam Physician* 75: 56–63, 2007.
14. DeNicola GM, Karreth FA, Humpton TJ, Gopinathan A, Wei C, Frese K, Mangal D, Yu KH, Yeo CJ, Calhoun ES, Scrimieri F, Winter JM, Hruban RH, Iacobuzio-Donahue C, Kern SE, Blair IA, and Tuveson DA. Oncogene-induced Nrf2 transcription promotes ROS detoxification and tumorigenesis. *Nature* 475: 106–109, 2011.
15. Egler RA, Fernandes E, Rothermund K, Sereika S, de Souza-Pinto N, Jaruga P, Dizdaroglu M, and Prochownik EV. Regulation of reactive oxygen species, DNA damage, and c-Myc function by peroxiredoxin 1. *Oncogene* 24: 8038–8050, 2005.
16. Fan J and Bertino JR. K-ras modulates the cell cycle via both positive and negative regulatory pathways. *Oncogene* 14: 2595–2607, 1997.
17. Fujii J and Ikeda Y. Advances in our understanding of peroxiredoxin, a multifunctional, mammalian redox protein. *Redox Rep* 7: 123–130, 2002.
18. Graves JA, Metukuri M, Scott D, Rothermund K, and Prochownik EV. Regulation of reactive oxygen species homeostasis by peroxiredoxins and c-Myc. *J Biol Chem* 284: 6520–6529, 2009.
19. Halilovic E, She QB, Ye Q, Pagliarini R, Sellers WR, Solit DB, and Rosen N. PIK3CA mutation uncouples tumor growth and cyclin D1 regulation from MEK/ERK and mutant KRAS signaling. *Cancer Res* 70: 6804–6814, 2010.
20. Heneberg P. Use of protein tyrosine phosphatase inhibitors as promising targeted therapeutic drugs. *Curr Med Chem* 16: 706–733, 2009.
21. Hofmann B, Hecht HJ, and Flohe L. Peroxiredoxins. *Biol Chem* 383: 347–364, 2002.
22. Homma S, Ishii Y, Morishima Y, Yamadori T, Matsuno Y, Haraguchi N, Kikuchi N, Satoh H, Sakamoto T, Hizawa N, Itoh K, and Yamamoto M. Nrf2 enhances cell proliferation and resistance to anticancer drugs in human lung cancer. *Clin Cancer Res* 15: 3423–3432, 2009.
23. Immenschuh S and Baumgart-Vogt E. Peroxiredoxins, oxidative stress, and cell proliferation. *Antioxid Redox Signal* 7: 768–777, 2005.
24. Jemal A, Siegel R, Xu J, and Ward E. Cancer statistics, 2010. *CA Cancer J Clin* 60: 277–300, 2010.
25. Joshi G, Aluise CD, Cole MP, Sultana R, Pierce WM, Vore M, St Clair DK, and Butterfield DA. Alterations in brain antioxidant enzymes and redox proteomic identification of oxidized brain proteins induced by the anti-cancer drug adriamycin: implications for oxidative stress-mediated chemobrain. *Neuroscience* 166: 796–807, 2010.
26. Kerkhoff E and Rapp UR. Cell cycle targets of Ras/Raf signalling. *Oncogene* 17: 1457–1462, 1998.
27. Kim HJ, Chae HZ, Kim YJ, Kim YH, Hwangs TS, Park EM, and Park YM. Preferential elevation of Prx I and Trx expression in lung cancer cells following hypoxia and in human lung cancer tissues. *Cell Biol Toxicol* 19: 285–298, 2003.
28. Kim JH, Bogner PN, Baek SH, Ramnath N, Liang P, Kim HR, Andrews C, and Park YM. Up-regulation of peroxiredoxin 1 in lung cancer and its implication as a prognostic and therapeutic target. *Clin Cancer Res* 14: 2326–2333, 2008.
29. Kim YJ, Ahn JY, Liang P, Ip C, Zhang Y, and Park YM. Human prx1 gene is a target of Nrf2 and is up-regulated by hypoxia/reoxygenation: implication to tumor biology. *Cancer Res* 67: 546–554, 2007.
30. Kim YJ, Lee WS, Ip C, Chae HZ, Park EM, and Park YM. Prx1 suppresses radiation-induced c-Jun NH2-terminal kinase signaling in lung cancer cells through interaction with the glutathione S-transferase Pi/c-Jun NH2-terminal kinase complex. *Cancer Res* 66: 7136–7142, 2006.
31. Kim YS, Lee HL, Lee KB, Park JH, Chung WY, Lee KS, Sheen SS, Park KJ, and Hwang SC. Nuclear factor E2-related factor 2 dependent overexpression of sulfiredoxin and peroxiredoxin III in human lung cancer. *Korean J Intern Med* 26: 304–313, 2011.
32. Klein EA and Assoian RK. Transcriptional regulation of the cyclin D1 gene at a glance. *J Cell Sci* 121: 3853–3857, 2008.
33. Le Belle JE, Orozco NM, Paucar AA, Saxe JP, Mottahedeh J, Pyle AD, Wu H, and Kornblum HI. Proliferative neural stem cells have high endogenous ROS levels that regulate self-renewal and neurogenesis in a PI3K/Akt-dependant manner. *Cell Stem Cell* 8: 59–71, 2011.
34. Lee S, Choi H, Kim E, Kim H, Park YH, Yu DY, Yoon SJ, Kim J, Sheen Y, Park SN, and Yoon DY. Melphalan inhibits adenoma development through modulating the expression of K-ras-specific markers in K-ras Tg mice. *Int J Oncol* 37: 219–228, 2010.
35. Lee SH, Hu LL, Gonzalez-Navajas J, Seo GS, Shen C, Brick J, Herdman S, Varki N, Corr M, Lee J, and Raz E. ERK activation drives intestinal tumorigenesis in Apc(min/+) mice. *Nat Med* 16: 665–670, 2010.
36. Li L, Shoji W, Oshima H, Obinata M, Fukumoto M, and Kanno N. Crucial role of peroxiredoxin III in placental antioxidant defense of mice. *FEBS Lett* 582: 2431–2434, 2008.
37. Liu JJ, Chao JR, Jiang MC, Ng SY, Yen JJ, and Yang-Yen HF. Ras transformation results in an elevated level of cyclin D1 and acceleration of G1 progression in NIH 3T3 cells. *Mol Cell Biol* 15: 3654–3663, 1995.
38. Martindale JL and Holbrook NJ. Cellular response to oxidative stress: signaling for suicide and survival. *J Cell Physiol* 192: 1–15, 2002.
39. Mitsudomi T, Viallet J, Mulshine JL, Linnoila RI, Minna JD, and Gazdar AF. Mutations of ras genes distinguish a subset of non-small-cell lung cancer cell lines from small-cell lung cancer cell lines. *Oncogene* 6: 1353–1362, 1991.
40. Neumann CA and Fang Q. Are peroxiredoxins tumor suppressors? *Curr Opin Pharmacol* 7: 375–380, 2007.
41. Neumann CA, Krause DS, Carman CV, Das S, Dubey DP, Abraham JL, Bronson RT, Fujiwara Y, Orkin SH, and Van Etten RA. Essential role for the peroxiredoxin Prdx1 in erythrocyte antioxidant defence and tumour suppression. *Nature* 424: 561–565, 2003.
42. Palande K, Roovers O, Gits J, Verwijmeren C, Iuchi Y, Fujii J, Neel BG, Karisch R, Tavernier J, and Touw IP. Peroxiredoxin-controlled G-CSF signalling at the endoplasmic reticulum-early endosome interface. *J Cell Sci* 124: 3695–3705, 2011.
43. Papaiahgari S, Zhang Q, Kleeberger SR, Cho HY, and Reddy SP. Hyperoxia stimulates an Nrf2-ARE transcriptional response via ROS-EGFR-PI3K-Akt/ERK MAP kinase

signaling in pulmonary epithelial cells. *Antioxid Redox Signal* 8: 43–52, 2006.
44. Park JH, Kim YS, Lee HL, Shim JY, Lee KS, Oh YJ, Shin SS, Choi YH, Park KJ, Park RW, and Hwang SC. Expression of peroxiredoxin and thioredoxin in human lung cancer and paired normal lung. *Respirology* 11: 269–275, 2006.
45. Park SY, Yu X, Ip C, Mohler JL, Bogner PN, and Park YM. Peroxiredoxin 1 interacts with androgen receptor and enhances its transactivation. *Cancer Res* 67: 9294–9303, 2007.
46. Peeper DS, Upton TM, Ladha MH, Neuman E, Zalvide J, Bernards R, DeCaprio JA, and Ewen ME. Ras signalling linked to the cell-cycle machinery by the retinoblastoma protein. *Nature* 386: 177–181, 1997.
47. Rosseland CM, Wierod L, Flinder LI, Oksvold MP, Skarpen E, and Huitfeldt HS. Distinct functions of H-Ras and K-Ras in proliferation and survival of primary hepatocytes due to selective activation of ERK and PI3K. *J Cell Physiol* 215: 818–826, 2008.
48. Schumacker PT. Reactive oxygen species in cancer cells: live by the sword, die by the sword. *Cancer Cell* 10: 175–176, 2006.
49. Shi X, Zhang Y, Zheng J, and Pan J. Reactive oxygen species in cancer stem cells. *Antioxid Redox Signal* 16: 1215–1228, 2012.
50. Shinohara M, Shang WH, Kubodera M, Harada S, Mitsushita J, Kato M, Miyazaki H, Sumimoto H, and Kamata T. Nox1 redox signaling mediates oncogenic Ras-induced disruption of stress fibers and focal adhesions by down-regulating Rho. *J Biol Chem* 282: 17640–17648, 2007.
51. Slebos RJ, Kibbelaar RE, Dalesio O, Kooistra A, Stam J, Meijer CJ, Wagenaar SS, Vanderschueren RG, van Zandwijk N, Mooi WJ, *et al.* K-ras oncogene activation as a prognostic marker in adenocarcinoma of the lung. *N Engl J Med* 323: 561–565, 1990.
52. Stresing V, Baltziskueta E, Rubio N, Blanco J, Arriba M, Valls J, Janier M, Clezardin P, Sanz-Pamplona R, Nieva C, Marro M, Dmitri P, and Sierra A. Peroxiredoxin 2 specifically regulates the oxidative and metabolic stress response of human metastatic breast cancer cells in lungs. *Oncogene* 32: 724–735, 2013.
53. Sun HN, Kim SU, Huang SM, Kim JM, Park YH, Kim SH, Yang HY, Chung KJ, Lee TH, Choi HS, Min JS, Park MK, Kim SK, Lee SR, Chang KT, Lee SH, Yu DY, and Lee DS. Microglial peroxiredoxin V acts as an inducible anti-inflammatory antioxidant through cooperation with redox signaling cascades. *J Neurochem* 114: 39–50, 2010.
54. Vachtenheim J. Occurrence of ras mutations in human lung cancer. Minireview. *Neoplasma* 44: 145–149, 1997.
55. Vaque JP, Navascues J, Shiio Y, Laiho M, Ajenjo N, Mauleon I, Matallanas D, Crespo P, and Leon J. Myc antagonizes Ras-mediated growth arrest in leukemia cells through the inhibition of the Ras-ERK-p21Cip1 pathway. *J Biol Chem* 280: 1112–1122, 2005.
56. Wang XQ, Li H, Van Putten V, Winn RA, Heasley LE, and Nemenoff RA. Oncogenic K-Ras regulates proliferation and cell junctions in lung epithelial cells through induction of cyclooxygenase-2 and activation of metalloproteinase-9. *Mol Biol Cell* 20: 791–800, 2009.
57. Weinberg F, Hamanaka R, Wheaton WW, Weinberg S, Joseph J, Lopez M, Kalyanaraman B, Mutlu GM, Budinger GR, and Chandel NS. Mitochondrial metabolism and ROS generation are essential for Kras-mediated tumorigenicity. *Proc Natl Acad Sci U S A* 107: 8788–8793, 2010.
58. Xia C, Meng Q, Liu LZ, Rojanasakul Y, Wang XR, and Jiang BH. Reactive oxygen species regulate angiogenesis and tumor growth through vascular endothelial growth factor. *Cancer Res* 67: 10823–10830, 2007.
59. Zhang B, Su Y, Ai G, Wang Y, Wang T, and Wang F. Involvement of peroxiredoxin I in protecting cells from radiation-induced death. *J Radiat Res (Tokyo)* 46: 305–312, 2005.
60. Zhang B, Wang Y, and Su Y. Peroxiredoxins, a novel target in cancer radiotherapy. *Cancer Lett* 286: 154–160, 2009.

Address correspondence to:
Dr. Dae-Yeul Yu
Disease Model Research Laboratory
Aging Research Center
Korea Research Institute of Bioscience and Biotechnology
125 Gwahak-ro, Yuseong-gu
Daejeon 305-806
Korea

E-mail: dyyu10@kribb.re.kr

Date of first submission to ARS Central, November 20, 2011; date of final revised submission, October 17, 2012; date of acceptance, November 2, 2012.

Abbreviations Used

CCK-8 = cell counting kit-8
DMSO = dimethyl sulfoxide
ERK = extracellular signal-regulated kinase
HO-1 = heme oxygenase-1
Keap1 = kelch-like ECH-associated protein 1
MEFs = mouse embryonic fibroblasts
MEK = mitogen-activated protein kinase kinase
NAC = N-acetyl L-cysteine
Nrf2 = nuclear erythroid 2-related factor 2
NSCLC = nonsmall-cell lung cancer
Prx = peroxiredoxin
PTP = protein tyrosine phosphatase
ROS = reactive oxygen species
Tg = transgenic
WT = wild type